Vis Comput
DOI 10.1007/s00371-013-0875-4

ORIGINAL ARTICLE

Physiological inverse tone mapping based on retina response

Yongqing Huo · Fan Yang · Le Dong · Vincent Brost

Abstract The mismatch between the Low Dynamic Range (LDR) content and the High Dynamic Range (HDR) display arouses the research on inverse tone mapping algorithms. In this paper, we present a physiological inverse tone mapping algorithm inspired by the property of the Human Visual System (HVS). It first imitates the retina response and deduce it to be local adaptive; then estimates local adaptation luminance at each point in the image; finally, the LDR image and local luminance are applied to the inversed local retina response to reconstruct the dynamic range of the original scene. The good performance and high-visual quality were validated by operating on 40 test images. Comparison results with several existing inverse tone mapping methods prove the conciseness and efficiency of the proposed algorithm.

Y. Huo (✉) · F. Yang · V. Brost
LE2I-CNRS 6306 Laboratory, University of Burgundy,
Dijon 21078, France
e-mail: hyq980132@163.com

F. Yang
e-mail: fanyang@u-bourgogne.fr

V. Brost
e-mail: vincent.brost@u-bourgogne.fr

Y. Huo
School of Communication and Information Engineering,
University of Electronic Science and Technology of China,
Chengdu 611731, China

L. Dong
School of Computer Science and Engineering,
University of Electronic Science and Technology of China,
Chengdu 611731, China

Published online: 13 September 2013

Keywords High Dynamic Range · Human visual system · Inverse tone mapping · Image quality metric · Local adaptive luminance

1 Introduction

Recently developed High Dynamic Range (HDR) monitors have greatly extended the limited dynamic range of conventional displays, and can simultaneously present bright highlights and dark shadows, so they have gained significant interest in industry. The availability and advancement of HDR displays make it necessary to solve how to show the large existing Low Dynamic Range (LDR) images and videos on HDR monitors. In this context, a number of algorithms for expanding LDR content to HDR image have been introduced; they were called inverse/reverse tone mapping [1].

Among these algorithms, Akyuz et al. [2] presented a simple linear expansion method, which indicates that LDR image does not necessarily require sophisticated treatment to produce a compelling HDR experience. Simply boosting the range of an LDR image linearly to fit the HDR display can equal or even surpass the appearance of a true HDR image. This method works well under the hypothesis that the input image has no compression artifacts and artistically captured. Focusing on the images with large saturated areas, Masia et al. [3] proposed another simple global expansion method based on γ transmission.

The more experienced algorithms detect saturated areas and expand them more sophisticatedly. Meylan et al. [4] introduced a piece-wise linear mapping function that allocates more range to those highlights in image. Didyk et al. [5] gave an interactive algorithm that classified a scene into diffuse, reflections and light sources, enhancing only reflec-

tions and light sources. Another interactive method [6] divided images into objects of interest and background, assigning more dynamic range to objects of interest by applying piece-wise linear function. Wang et al. [7] reconstructed the details of the incorrect-exposed regions by copying the texture in the correct-exposed regions. Banterle et al. [8–10] proposed a general framework to map LDR content with saturated areas. The framework first maps the LDR content to middle dynamic range by iTMO (inverse Tone Mapping Operator), then performs an expand-map to reconstruct lost luminance profiles in the saturated areas of the image and attenuate the quantization and compression artifacts. In a similar manner, Rempel et al. [11] computed a brightness enhancement mapping function to scale the contrast that has been linearly mapped to medium range. Kovaleski et al. [12] substituted a bilateral filter for the combination of a Gaussian blur and an edge stopping function used by Rempel and colleagues.

Although the algorithms described above produce appealing results for a wide range of LDR contents, Aukyz et al.'s algorithm may not work well for images with low quality; Masia et al.'s γ expansion may be unsuitable for images with low key value, as the low key value potentially results in negative γ value, which will cause false results. Other algorithms perform sophisticated treatment to saturated areas or boost them largely; this introduces the possibility of making the image appear worse than before processing through the introduction of objectionable artifacts [3]; the large boosting to the bright image areas sometimes results in contouring artifacts for bright object.

In fact, because of the large difference between the luminance ranges of these two formats, the faithful reproduction of the HDR content from the LDR content is not possible in general. However, studies on Human Visual System (HVS) show that the perceived brightness of each point in a scene is not simply determined by its absolute luminance; instead, the electric signal generated by the cone and rod cells of the retina is transmitted through different layers of cells that introduce a complex, and not yet fully understood, sequence of spatial interactions, nonlinear mappings, and feedback mechanisms [13, 14]. One useful consequence of these mechanisms is that, in order to reproduce an image, it is not necessary to generate an identical or proportional luminance on the display device; by exploiting the characteristics of human vision, it is possible to process change in the image in order to amplify its dynamic range without producing a significant change in the visual sensation experienced by the observers [15].

In this paper, we propose a physiological inverse tone mapping algorithm that is able to produce high-quality HDR images with a very low computational complexity and a limited number of parameters. It belongs to the category of methods based upon the retina response, and the main novel contribution consists in the inverse and consideration of the local adaptive response of retina. This makes the proposed algorithm comply with the physiological perception procedure to light; furthermore, it minimizes the formation of artifacts, such as detail loss and contrast reversal that often occurs in existing methods. In our method, the local response is implemented by slightly shifting the global adaptation level based on the local information of each pixel. This manner considers simultaneously the general information of the whole image and the local characters at different pixel position.

This paper is organized as follows: The physiological response mechanism of HVS and an overview of the proposed system are given in Sect. 2. In Sect. 3, the mathematical model of physiological inverse tone mapping based on retina response is illustrated. Selected representative results of a comprehensive experimental evaluation are given in Sect. 4. Conclusions and further discussions are presented in the last section.

2 Backgrounds

2.1 Visual perception mechanism

The Human Visual System (HVS) is the most important system through which our brain gathers information about our surroundings, and forms one of the most complex physiological systems. It is capable of adapting to a great range of light, as the light intensity increases, the sensitivity of the HVS is decreased, which allows for operation over 10 orders of magnitude of light levels [16].

As shown in Fig. 1 [17], the first step of HVS to light is global perception, in which, the nonlinearity of lightness perception and the color perception happen simultaneously. Based on the fact that the HVS operates on multiple channels, each one tuned to different spatial frequency and orientation [18], the visual information is decomposed into

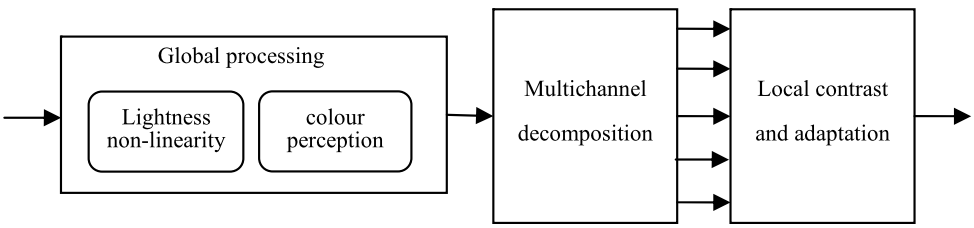

Fig. 1 Block diagram of a HVS model

Fig. 2 System framework

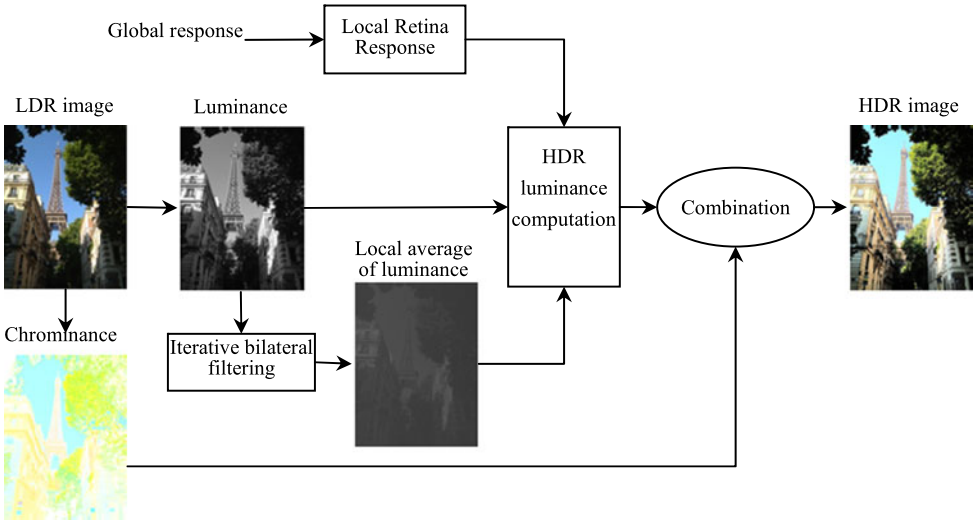

channels. Once the decomposition was done, local contrast mechanisms come into effect. In fact, the HVS response depends predominantly on local variations of luminance and very little on the absolute luminance value. In scene perception processes of the HVS, the global layout of the scene is caught in the first instance and the local contrasts are the focus in the following steps.

2.2 System overview

The proposed system belongs to the category of methods based upon the retina response and mainly consists of three processing modules, i.e., global response to local response of retina, local surrounding luminance computation, and the calculation of HDR image luminance. As shown in Fig. 2, the local response of retina is deduced from the global one and be used as the mathematical model in computing the HDR luminance. The input LDR image is first decomposed into luminance channel and chrominance channel, the local surrounding luminance is computed by the weighted average using iterative bilateral filter on the luminance image. Then the local surrounding luminance and the image luminance are performed on the local response of retina to compute the HDR luminance. Finally, the obtained luminance and the chrominance channel are combined to generate HDR image. The corresponding mathematical models and details outlined in Fig. 2 are elaborated in the next section.

3 Physiological inverse tone mapping algorithm based on retina response

3.1 Algorithm description

Because of its adaptation property, the eye is more sensitive to changes in light level than to a steady input. When a space-independent pulse of light is shone on the entire eye, the retina responds with a large-amplitude signal at the beginning followed by a decrease to a lower plateau. That means the retina first accommodates to some luminance value; then perceives images in a rather small dynamic range around this luminance value. Thus, as illustrated in above section, the basic process of our vision is a global tone mapping to the entire scene. This global function can be described by the relationship between the retina response and stimulus light intensity [19]:

$$\frac{R}{R_{\max}} = \frac{I^n}{I^n + \sigma^n} \tag{1}$$

where R is the retina response, $R_{\max}$ is the maximum response, and I is the light intensity. σ is the global adaptation level, which represents the luminance required to generate a response one-half of the amplitude of $R_{\max}$. The parameter n is a sensitivity control exponent.

It has been proved that the absolute brightness information is of secondary importance to HVS and tends to be largely discarded on very early stages of visual processing through mechanisms of brightness constancy. Local contrasts are used instead to convey the wealth of information about the scene [20]. Hence, the more proper description of retina response should be a local mapping. The local adaptive property can be realized by slightly changing the adaptation level σ depending on the surrounding light intensity [21]. Let I_p be the intensity of pixel p in a HDR image; by defining a spatially variant value $\Delta\sigma_p$, which is a small change in σ, according to (1), the output LDR image R_p can be described as

$$R_p = R_{\max} \frac{I_p^n}{I_p^n + (\sigma + \Delta\sigma_p)^n} \tag{2}$$

where $R_{\max}$ is the maximum value of the LDR output. If we expand the term $(\sigma + \Delta\sigma_p)^n$ to be $\sigma^n + n \cdot \sigma^{n-1} \cdot (\Delta\sigma_p) +$

$n \cdot \sigma \cdot (\Delta\sigma_p)^{n-1} + \cdots + (\Delta\sigma_p)^n$, and replace the sum of the second term to the last term in the expanded form with $\Delta\sigma_p''$, (2) can be rewritten as

$$R_p = R_{\max} \frac{I_p^n}{I_p^n + \sigma^n + \Delta\sigma_p''} \tag{3}$$

where $\Delta\sigma_p''$ indicates a displacement from the global adaptation level, it can be obtained by the difference between the original image intensity and its surrounding image intensity [21]. Let I_p and $I_{s,p}$ be the intensity of pixel p and its surrounding intensity in HDR image respectively, we have

$$R_p = R_{\max} \frac{I_p^n}{I_{s,p}^n + \sigma^n} \tag{4}$$

Usually, for LDR to HDR expansion, only the luminance channel is processed, the chrominance channels are intact. So, we operate the local function (4) on the luminance channel:

$$L_l = L_{\max,l} \frac{L_h^n}{L_{s,h}^n + \sigma^n} \tag{5}$$

where L_l and $L_{\max,l}$ are the luminance and the maximum luminance of LDR image respectively, L_h and $L_{s,h}$ correspond to the luminance and the surrounding luminance of HDR image.

The above describes the local tone compression procedure. For inverse tone mapping, i.e., tone expansion, we need to get L_h from (5):

$$L_h = \left(\frac{L_l}{L_{\max,l}} \left(L_{s,h}^n + \sigma^n \right) \right)^{\frac{1}{n}} \tag{6}$$

In (6), L_l and $L_{\max,l}$ can be directly obtained from LDR image. The following will describe how to set parameters n, σ and $L_{s,h}$.

3.2 Parameters setting

There are three parameters need to be determined. The value of parameter n is determined by the time of test flashes while capturing the image; parameter σ is the value of luminance that causes the half-maximum response and it depends on the state of global, local, and temporal adaptation; parameter $L_{s,h}$ is the surrounding luminance value of each pixel in the image. There is no direct correlation between these parameters, we can set them separately.

The sensitivity parameter n was discussed in the literature [19] that has a value generally between 0.7 (long test flashes) and 1.0 (short test flashes). We carried out a lot of experiments by increasing the value of n gradually from 0.7 to 1.0; the results suggest that $n = 0.86$ is better for our test images.

The parameters σ and $L_{s,h}$ are information related to the luminance of HDR image, however, only the LDR image is known. Thus, based on the assumption that the maximum luminance 255 of a LDR image will be mapped to the maximum luminance $L_{\max,h}$ of the HDR display, we first compute the corresponding σ_l and $L_{s,l}$ of the LDR image, then substitute $\sigma_l * L_{\max,h}/255$ and $L_{s,l} * L_{\max,h}/255$ for σ and $L_{s,h}$.

The σ_l is obtained using the log-average luminance:

$$\sigma_l = \exp\left(\frac{1}{N} \left(\sum_{x,y} \log\big(L(x,y) + \theta\big) \right) \right) \tag{7}$$

where $L(x, y)$ is the pixel luminance at (x, y), θ is a small nonnegative value, and N is the number of pixels in the image.

There are various ways to compute the surrounding luminance. We use the weighted average $BF \otimes L_l$ to portray the $L_{s,l}$, BF is bilateral filter, which is introduced by Durand and Dorsey [22]. It is known as an edge-preserving smoothing operator that effectively blurs an image, but keeps sharp edges intact. We use iterative bilateral filter for obtaining more proper surrounding luminance.

The filtered output $L_{s,l}$ of the jth iteration for a pixel q is as

$$L_{s,l,q}^0 = L_{l,q} \tag{8}$$

$$L_{s,l,q}^j = \frac{1}{k_q^j} \sum_{p \subset \Omega} f_{\sigma_m^j}(p-q) g_{\sigma_d^j}\big(L_{s,l,p}^{j-1} - L_{s,l,q}^{j-1}\big) L_{s,l,p}^{j-1} \tag{9}$$

where $j = 1, 2$ is the iterative number, $L_{l,q}$ is the luminance of the original LDR image at pixel q; k_q^j is a normalization term:

$$k_q^j = \sum_{p \subset \Omega} f_{\sigma_m^j}(p-q) g_{\sigma_d^j}\big(L_{sl,p}^{j-1} - L_{sl,q}^{j-1}\big) \tag{10}$$

where σ_m is the standard deviation for a Gaussian f in the spatial domain such as

$$f_{\sigma_m}\big(q | q = (x,y)\big) = K_m \exp\left\{ -\frac{x^2 + y^2}{\sigma_m^2} \right\} \tag{11}$$

here, K_m is a normalization factor and Ω is the whole image. σ_d is the standard deviation for a Gaussian g in the range domain. The experiments suggest that for our test images the parameters σ_m^1 and σ_m^2 set to 16 and 10, and σ_d^1 and σ_d^2 set to 0.3 and 0.1 are appropriate.

4 Experiments and evaluations

We implemented the proposed algorithm with Matlab2011b on an Intel Core i5-2520M CPU @ 2.5 GHz, 4.00 GB RAM,

Fig. 3 A subset of test images, from left-top to right-bottom: Boat, Leaf, Landscape, Lucerne, Building, Park, and Sky

win32 system. The maximum illumination of the HDR monitor is set to 3000 cd/m^2, according to Brightside's 37″ HDR monitor. A wide range of images are used to test the performance of the system, these images represent overexposed and underexposed scenes in various lighting conditions, from very dark to very bright. Figure 3 shows a subset of these test images.

4.1 Algorithm implementations

In order to test and validate the physiological inverse tone mapping model, we operated on 40 images and compared to two global and three local methods using an image quality metric. Here, we give brief description of these algorithms and their implementation (for a detailed explanation of the parameters in these algorithms, the reader can refer to the original papers).

(1) The linear expansion [2] is one of the global methods. It is the most simple among the compared algorithms and its computational complexity is the lowest.

(2) Banterle et al.'s operator [8] is a local one. It first expands the image to medium range through inverting the TMO proposed by Reinhard et al. [23] as

$$L_{m,h} = \frac{L_{\max} L_{\text{white}}}{2}\left[L_l - 1 + \sqrt{(1-L_l)^2 + 4 \times L_l / L_{\text{white}}^2}\right]$$

where $L_{m,h}$ is the luminance after medium expanding, L_l is the luminance of LDR image, $L_{\max}$ is the maximum luminance value expected for the inverse tone mapped image, and L_{white} is the smallest luminance value that will be mapped to white.

Then the saturated areas are found using median cut; finally based on the density estimation of the saturated areas, an expand-map is computed to combine the original LDR image and the expanded medium range image. In the implementation, when generating the expand-map, the radius of the density estimation is 16 pixels; the threshold is 4 light sources and the number of generated light sources for a median cut sampling is $4 \times 2^{\log}_{2^{(\min(r,c))}}$, r and c are the height and width of the input image.

(3) LDR2HDR [11] first maps pixel values into linear luminance, then a brightness enhancement function together with an edge-stopping function are computed and applied to increase brightness in saturated regions. For this algorithm, the parameters used are 150 pixels for the standard deviation of the large Gaussian blur applied to the mask, a rescaling factor $\alpha = 4$, and a gradient image baseline width for divided differences of 5 pixels. The maximum iteration number for the flood fill is set to 1000, a 5×5-pixel kernel for the anti-aliasing blur, and a 4-pixel radius for the open operator are used to clean up the final edge stopping function.

(4) Meylan et al.'s method [4] divided image into specular and diffuse components, a tone scale function composed of two slopes is used to allocate different percentage of the maximum display luminance to different components. For this algorithm, the percentage ρ value is took as 0.67; the size of the filters for computing two thresholds are $(m+1) \times (m+1)$ and $(2m+1) \times (2m+1)$, respectively, $m = \max(r, c)/50$, r and c is the height and width of input image. An iterative erosion and dilatation with 3 steps are used to obtain the binary mask for detecting highlight specular; the size of average filter for smooth is 5×5.

(5) The γ expansion [3] is another global method, the γ value is determined by image key value, and other two parameters a and b. In the implementation, a and b are set to 10.44 and −6.282, respectively, as in the original paper.

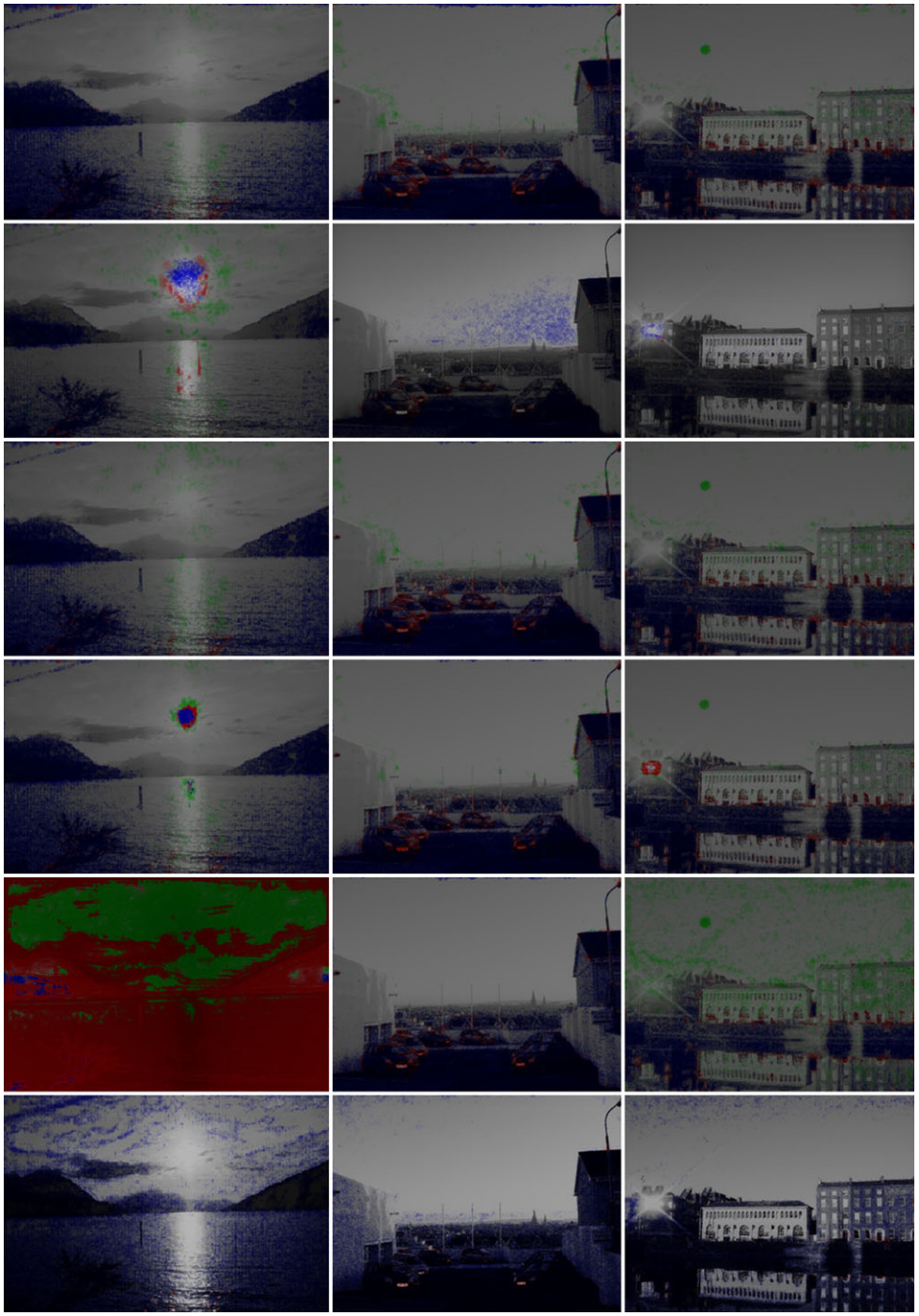

Fig. 4 Comparison results of six algorithms with the image quality metric of Aydin et al. [24]: the reference LDR images are Lucerne, Park, and Building in Fig. 3. In each group, from top to bottom: Linear expansion, Banterle et al.'s operator, LDR2HDR, Meylan et al.'s method, γ expansion and proposed algorithm. *Red*, *green*, and *blue* identify contrast reversal, loss of visible contrast, and amplification of invisible contrast, respectively. Our algorithm amplifies more detail, and causes least contrast loss and reversals

4.2 Evaluation experiments

We choose an image quality metric introduced by Aydin et al. [24] to assess the quality of the generated HDR images (the original LDR image as reference image). This metric identifies visible distortions between two images and be independent of the dynamic range of image. The result image generated by this metric is a summary image with red, green, and blue pixels, which determines whether contrast in the image has been reversed, reduced, or improved. The color is determined for each pixel depending on the highest contributor. The red pixels mean that the contrast for these pixels are reversed (the contrast polarity is reversed in the compared image with respect to the reference image); the green pixels imply that the contrast for these pixels are lost (visible contrast in the reference image becomes invisible in the compared image); the blue pixels denote that the contrast for these pixels are amplified (invisible contrast in the

Table 1 Red, green, and blue percentages of metric results for subset images in Fig. 3: Larger red percentage means more contrast reversal, larger green percentage denotes more contrast loss, and larger blue percentage indicates more contrast amplification

Percentage		Images							
		Boat	Leaf	Landscape	Lucerne	Building	Park	Sky	Average
red	Akyuz	5.99	18.82	2.44	2.03	9.15	4.9	9.48	7.544
	Banterle	5.14	7.53	0.63	1.18	3.26	2.8	3.84	3.884
	Rempel	4.31	17.36	1.6	2.09	8.52	4.94	4.73	6.221
	Meylan	2.62	16.8	1.54	1.97	7.44	4.33	5.03	5.676
	Masia	0.31	19.57	1.28	73.15	6.23	3.02	0.72	14.9
	Proposed	0.25	4.59	0.36	0.076	1.25	0.76	0.85	**1.162**
green	Akyuz	8.09	50.54	4.72	23.08	17.17	16.9	20.32	20.11
	Banterle	4.05	1.72	1.32	17.5	5.25	1.58	0.76	4.597
	Rempel	37.09	63.31	42.66	23.23	25.9	14.46	32.91	34.51
	Meylan	19.4	48.41	18.74	15.63	13.11	6.55	17.81	19.95
	Masia	99.36	78.85	2.43	26.12	61.7	0.74	0.039	38.46
	Proposed	0.2	0.37	0.13	0.054	0.19	0.033	0.061	**0.148**
blue	Akyuz	17.12	3.37	21.79	10.48	31.01	34.91	26.91	20.79
	Banterle	20.93	7.57	33.54	31.92	32.59	46.39	29.04	28.85
	Rempel	6.96	3.26	18.61	10.43	28.73	34.85	4.42	15.32
	Meylan	5.99	13.55	21.22	15.09	31.44	37.23	5.56	18.58
	Masia	0.14	1.07	21.51	0.66	22.28	42.48	29.78	16.85
	Proposed	35.41	10.78	40.45	58.61	64.52	59.08	20.13	**41.28**

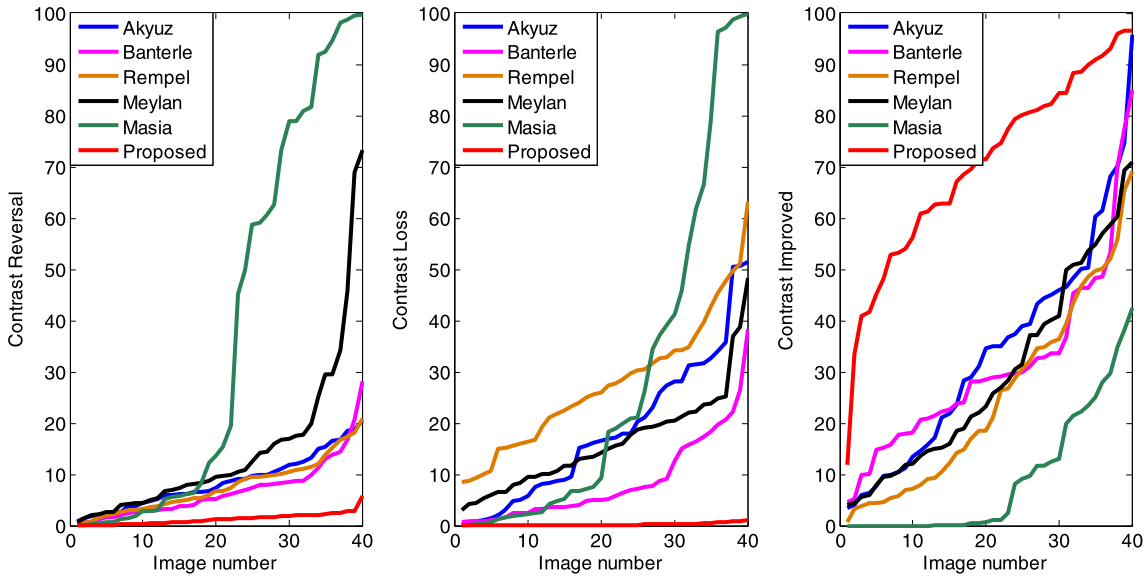

Fig. 5 From left to right: *red*, *green*, and *blue* percentages curve resulting from the comparison between forty test images (reference images) and the HDR images generated by six algorithms using the image quality metric of Aydin et al. [24]. The percentage values of each algorithm are sorted for comparison clarity. The proposed algorithm has maximum contrast amplified, minimum contrast reversal, and contrast loss

reference image becomes visible in the compared image). In our test, the original LDR images are reference images, the generated HDR images are compared images. Figure 4 shows some result images generated by the metric for six algorithms.

Furthermore, we compared the algorithms numerically by computing the percentage of red, green and blue pixels (the ratio of the red, green, and blue pixel number to the total number of image) of the result images obtained by the image quality metric. Table 1 gives their percentage values corre-

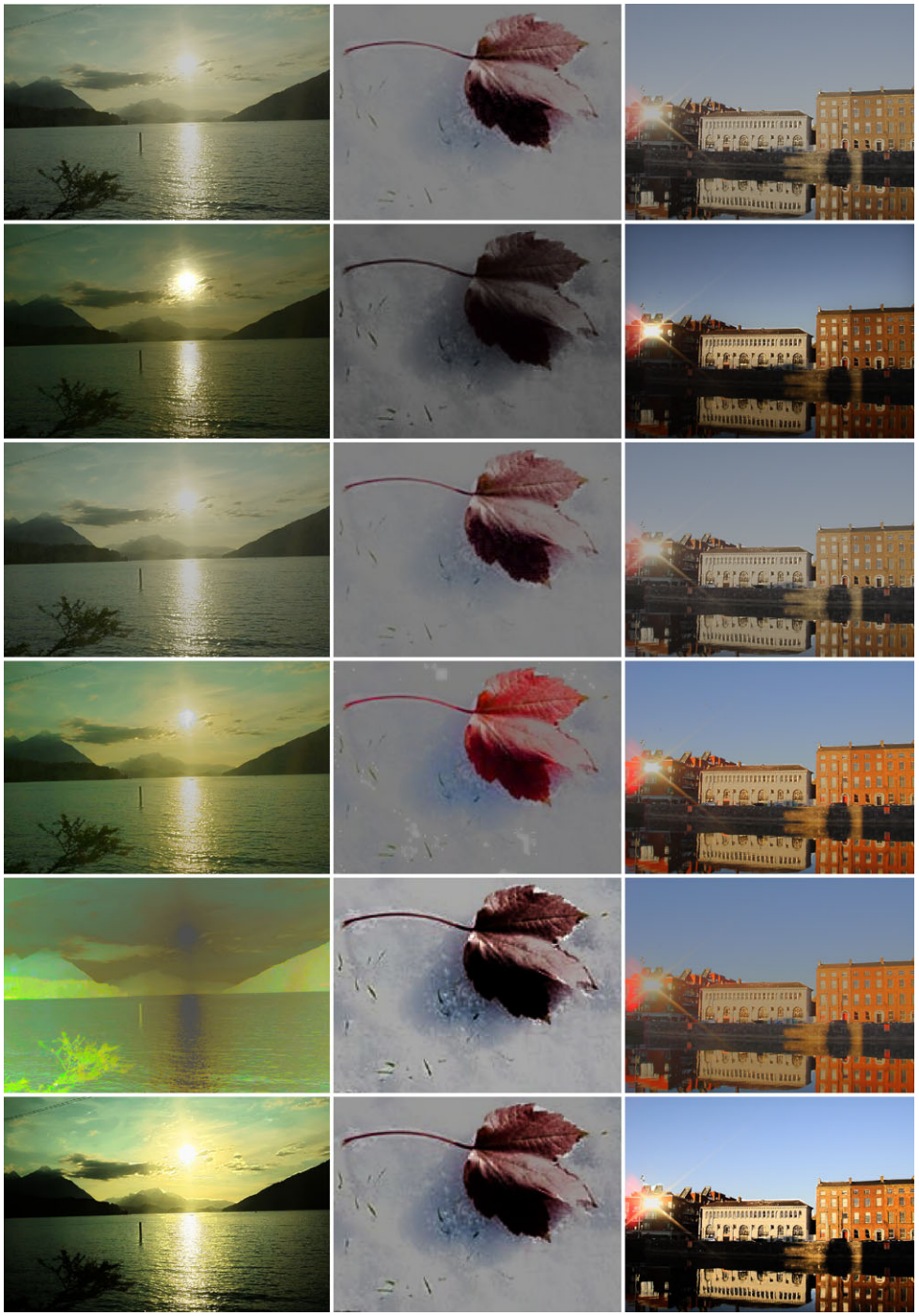

Fig. 6 Tone mapped images of six algorithms. In each group, from top to bottom: Linear expansion, Banterle et al.'s operator, LDR2HDR, Meylan et al.'s method, γ expansion, and proposed algorithm. All tone mapped versions are produced using Reinhard et al.'s TMO [23]

sponding to images in Fig. 3. Other percentage values of metric results for forty test images are computed and drawn in Fig. 5.

4.3 Results analysis and discussion

The experimental results show that our physiological scheme can generate high-quality result images with a very compact form as (6). Table 1 and Fig. 5 show that our algorithm has minimum red and green percentages, but maximum blue percentage, which means that it can obtain more contrast improvement with little negligible contrast loss and reversal than other compared algorithms; Fig. 4 testifies these results visually, in three metric result images of our method, there are no visible green pixels and tiny red pixels. These numerical results also show that the performance of Banterle et al.'s operator is the second in the six algorithms; the contrast reversal and contrast loss of the linear expansion

Table 2 Comparison of the running times of six algorithms: our algorithm has minimum running time among the local methods (Banterle's operator, LDR2HDR, Meylan's method)

Methods	Time (s)
Linear expansion	0.104
Banterle's operator	14.06
LDR2HDR	0.692
Meylan's method	0.570
γ expansion	0.324
Proposed algorithm	0.498

is between that of Meylan et al.'s method and LDR2HDR, but the contrast improvement of linear expansion is close to Banterle et al.'s algorithm. For γ expansion which focuses on expanding images with large saturated regions, for some test images which are not large saturated, its performance is undesirable.

The good performance of the proposed algorithm was also observed by the tone mapped version of the generated HDR images, which cannot be shown here directly because of limitations of the print medium. The tone mapped versions are generated by Reinhard et al.'s photographic operator [23], three of them for all algorithms are offered in Fig. 6; the corresponding original images were captured at different luminance conditions (Lucerne, Leaf, and Building in Fig. 3). These tone mapped images also imply that our algorithm works well and can obtain pleased images. The rebarbative results of γ expansion also suffer from the low key value of the test images. Concerning the computational complexity, Table 2 compares the running time of the different algorithms using the test image Sky in Fig. 3 with a resolution of 960×540 pixels. The algorithms were run on the platform that we have described in the beginning of Sect. 3. The table implies that except the global methods, our algorithm has minimum computational complexity with its fast speed and compact mathematical form among the local methods considered in this comparison. Although the running speed of our method is little slower than the global ones, with its high-quality result HDR images and good applicability, the general performance of our approach is better than the global ones.

The results of the experiments show that our scheme does not introduce objectionable artifacts and contouring artifacts at the edges of bright objects. These artifacts are usually introduced by the use of different expansion methods to the saturated and nonsaturated areas, and large boosting to the bright objects. However, unlike the algorithms considered in our experiments, we expand the saturated areas and nonsaturated areas using the same mathematical model. Furthermore, the expansion of each pixel is not only related to the luminance value of itself, but also the luminance values of its surrounding pixels. For a pixel at the edges of the bright objects or between the saturated and nonsaturated areas, because some of its surrounding pixels are dimmer than it, its surrounding luminance value is smaller than its value. This prevents the large boosting to the edge pixels and avoids contouring artifacts.

The excellent performance of the proposed algorithm owes to its physiological property and the use of local adaptive luminance. The physiological property intrinsically enables the algorithm to imitate the inverse of the procedure that the retina perceives the real-world scene, which makes the generated HDR image approximates to the real-world scene as far as possible. The consideration of local adaptive luminance guarantees the enhancement to local details, simultaneously eliminates special treatment to the saturated regions, which favors the conciseness of the algorithm. In brief, the simulation results prove that the proposed algorithm has good performance for all kinds of tested ill-exposed images, low computational complexity, and limited parameters.

5 Conclusions

In this paper, we proposed a new inverse tone mapping approach inspired by the adaptation property of HVS. It is capable of generating high-visual quality HDR images with low computational complexity and limited number of parameters compared to some existing algorithms. The way to expand the retina response to be local adaptive ensures that the proposed approach resolves the two most important issues in inverse tone mapping: enhancing local contrast and preserving the details. Evaluation results show the high performance and low computational complexity of our algorithm. The numerical and visual results suggest that it obtains more contrast improvement with least contrast loss and reversal than other recent algorithms. The computational efficiency combined with the high visual quality of the result images makes the proposed method attractive. In the following work, we will exploit more sophisticated ways for estimating the parameters to make the algorithm more compact. The conciseness and efficiency make the algorithm be suitable for hardware implementation, which is the ongoing work for platform integration.

Acknowledgements This work was supported in part by the Postdoctoral Funds of the Burgundy Region of France, in part by the Fundamental Research Funds for the Central Universities (No. ZYGX2011J004), in part by the National Natural Science Foundation of China under Grant 61003123, and in part by the Fundamental Research Funds for the Central Universities (No. ZYGX2011X014).

References

1. Banterle, F., Debattista, K., Artusi, A., Pattanaik, S., Myszkowski, K., Ledda, P., Bloj, M., Chalmers, A.: High dynamic range imaging and low dynamic range expansion for generating HDR content. Comput. Graph. Forum **28**(8), 2343–2367 (2009)
2. Akyuz, O., Fleming, R., Riecke, B.E., Reinhard, E., Bulthoff, H.H.: Do HDR displays support LDR content? A psychophysical evaluation. ACM Trans. Graph. **26**(3), 1–7 (2007)
3. Masia, B., Agustin, S., Fleming, R.W., Sorkine, O., Gutierrez, D.: Evaluation of reverse tone mapping through varying exposure conditions. ACM Trans. Graph. **28**(5), 1–8 (2009)
4. Meylan, L., Daly, S., Susstrunk, S.: The reproduction of specular highlights on high dynamic range displays. In: Proceedings of the IST/SID 14th Color Imaging Conference, pp. 333–338. Society for Imaging Science and Technology (IS&T), Springfield (2006)
5. Didyk, P., Mantiuk, R., Hein, M., Seidel, H.P.: Enhancement of bright video features for hdr displays. Eurographics Symp. Render. **27**(4), 1265–1274 (2008)
6. Masia, B., Fleming, R., Sorkine, O., Gutierrez, D.: Selective reverse tone mapping. In: Proceedings of CEIG (2010)
7. Wang, L., Wei, L.-Y., Zhou, K., Guo, B., Shum, H.-Y.: High dynamic range image hallucination. In: Eurographics Symposium on Rendering (2007)
8. Banterle, F., Ledda, P., Debattista, K., Chalmers, A.: Inverse tone mapping. In: Proc. 4th International Conf. Computer Graphics and Interactive Techniques in Australasia and Southeast Asia, pp. 349–356. ACM, New York (2006)
9. Banterle, F., Ledda, P., Debattista, K., Chalmers, A., Bloj, M.: A framework for inverse tone mapping. Vis. Comput. (2007). doi:10.1007/s00371-007-0124-9
10. Banterle, F., Ledda, P., Debattista, K., Chalmers, A.: Expanding low dynamic range videos for high dynamic range applications. In: Proceedings of SCCG, pp. 349–356. ACM, New York (2008)
11. Rempel, A.G., Trentacoste, M., Seetzen, H., Young, H.D., Heidrich, W., Whitehead, L., Ward, G.: Ldr2hdr: on-the-fly reverse tone mapping of legacy video and photographs. ACM Trans. Graph. **26**(3), 39 (2007)
12. Kovaleski, R.P., Oliveira, M.M.: High quality brightness enhancement functions for real-time reverse tone mapping. Vis. Comput. (2009). doi:10.1007/s00371-009-0327-3
13. Keener, J., Sneyd, J.: Mathematical Physiology. Springer, New York (1998)
14. Dong, L., Su, J., Izquierdo, E.: Scene-oriented hierarchical classification of blurry and noisy images. IEEE Trans. Image Process. **21**(5), 2534–2545 (2012)
15. Guarnieri, G., Marsi, S., Ramponi, G.: High dynamic range image display with halo and clipping prevention. IEEE Trans. Image Process. **20**(5), 1351–1362 (2011)
16. Reinhard, E., Ward, G., Pattanaik, S., Debevec, P.: High Dynamic Range Imaging: Acquisition, Display and Image Based Lighting. Morgan Kaufmann, San Francisco (2005)
17. Boev, A., Poikela, M., Gotchev, A., Aksay, A.: Modelling of the Stereoscopic HVS (2012). http://www.google.fr/url?sa=t&rct=j&q=Modelling+of+the+Stereoscopic+HVS&source=web&cd=1&cad=rja&ved=0CCMQFjAA&url=http%3A%2F%2Fsp.cs.tut.fi%2Fmobile3dtv%2Fresults%2Ftech%2FD5.3_Mobile3DTV_v2.0.pdf&ei=PeOfUID5D5OzhAfZo4CgCA&usg=AFQjCNF5EgXz9c1HjtNWMwVZoAsoz6DgBA
18. Daugman, J.G.: Two dimensional spectral analysis of cortical receptive field profiles. Vis. Res. **20**(10), 847–856 (1980)
19. Dowling, J.E.: The Retina: An Approachable Part of the Brain. Belknap Press, Cambridge (1987)
20. Shapley, R., Enroth-Cugell, C.: Visual adaptation and retinal gain-controls. Prog. Retin. Eye Res. **3**, 263–346 (1984)
21. Horiuchi, T., Tominaga, S.: HDR image quality enhancement based on spatially variant retinal response. EURASIP J. Image Video Process. (2010). doi:10.1155/2010/438958
22. Durand, F., Dorsey, J.: Fast bilateral filtering for the display of high-dynamic-range images. In: Proceedings of SIGGRAPH, pp. 257–266. ACM, New York (2002)
23. Reinhard, E., Stark, M., Shirley, P., Ferwerda, J.: Photographic tone reproduction for digital images. ACM Trans. Graph. **21**(3), 267–276 (2002)
24. Aydin, T.O., Mantiuk, R., Myszkowski, K., Seidel, H.P.: Dynamic range independent image quality assessment. In: Proceedings SIGGRAPH, pp. 1–10. ACM, Los Angeles (2008)

Yongqing Huo received her B.S. degree in communication engineering in 2002, M.S. degree and Ph.D. degree in signal and information processing in 2005 and 2007 from the University of Electronic Science and Technology of China. She is currently an assistant professor with the college of communication and information engineering at University of Electronic Science Technology of China. And now she is proceeding on to her postdoctoral research in University of Burgundy. Her current research interests include image analysis and HDR image processing.

Fan Yang received the B.S. degree in electrical engineering from the University of Lanzhou, China, in 1982 and the M.S. (D.E.A.) (computer science) and Ph.D. degrees (image processing) from the University of Burgundy, France, in 1994 and 1998, respectively. She is currently a full professor and member of LE2I CNRS-UMR, Laboratory of Electronic, Computing, and Imaging Sciences at the University of Burgundy, France. Her research interests are in the areas of patterns recognition, neural network, motion estimation based on spatiotemporal Gabor filters, parallelism and real-time implementation, and more specifically, automatic face image processing algorithms and architectures. Professor Yang is a member of the French research group ISIS (Information, Signal, Images, and Vision); she livens up the theme C: Algorithm Architecture Adequation.

Le Dong received the Ph.D. degree from Queen Mary, University of London, London, UK. She is currently an Associate Professor of Computer Science with the University of Electronic Science and Technology of China, Chengdu, China. She has cochaired/costeered a number of conferences and workshops and has published more than 30 technical papers in relevant research fields. Her research areas include multimedia and computer vision, human-cloud interaction, pattern recognition, and artificial intelligence, particularly including biologically inspired framework. Professor Dong is a Member of ACM.

Vincent Brost received the Master Degree and Ph.D. degrees from University of Burgundy. He is currently an associate professor at the University of Burgundy and member of LE2I (Laboratory of Electronic, Computing, and Imaging), France. His research interests are in the areas of rapid prototyping system, VLIW architecture, and electronic devices.